OXFORD

Hubs and interaction: the brain's meta-loop

Cornelius Weiller[1,*], Marco Reisert[2,3], Pierre Levan[4], Jonas Hosp[1], Volker A. Coenen[3], and Michel Rijntjes[1]

[1]Department of Neurology and Clinical Neuroscience, Faculty of Medicine, University of Freiburg, Breisacherstrasse 64, D-79106 Freiburg i.Br., Germany
[2]Department of Medical Physics, Faculty of Medicine, University of Freiburg, Breisacherstrasse 64, D-79106 Freiburg i.Br., Germany
[3]Department of Stereotactic and Functional Neurosurgery, Faculty of Medicine, University of Freiburg, Breisacherstrasse 64, D-79106 Freiburg i.Br., Germany
[4]Department of Radiology, University of Calgary, 2500 University Drive NW, Calgary, Alberta T2N 1N4, Canada

*Corresponding author: Cornelius Weiller, Breisacherstrasse 64, D-79106 Freiburg i.Br., Germany. Email: cornelius.weiller@uniklinik-freiburg.de

We must reconcile the needs of the internal world and the demands of the external world to make decisions relevant to homeostasis, well-being, and flexible behavior. Engagement with the internal (eg interoceptive) world is linked to medial brain systems, whereas the extrapersonal space (eg exteroceptive) is associated with lateral brain systems. Using Human Connectome Project data, we found three association tracts connecting the action-related frontal lobe with perception-related posterior lobes. A lateral dorsal tract and a medial dorsal tract interact independently with a ventral tract at frontal and posterior hubs. The two frontal and the two posterior hubs are interconnected, forming a meta-loop that integrates lateral and medial brain systems. The four anatomical hubs correspond to the common nodes of the intrinsic cognitive brain networks such as the default mode network. These functional networks depend on the integration of both realms. Thus, the positioning of functional cognitive networks can be understood as the intersection of long anatomical association tracts. The strength of structural connectivity within lateral and medial brain systems correlates with performance on behavioral tests assessing theory of mind. The meta-loop provides an anatomical framework to associate neurological and psychiatric symptoms with functional and structural changes.

Keywords: association tracts; default mode network; heteromodal cortex; theory of mind.

Introduction

The foremost task of the brain is to reconcile the internal and external world (Mesulam 1987). To survive in a complex environment, we must anticipate the needs of the organism by simulating its interaction with the world, addressing those needs before they arise ("allostasis"), and we have to engage with the world in a flexible manner. (Raichle 2015; Schulkin and Sterling 2019; Johnson 2025). We have to merge the internal and external realms for mental imagery and self-reference, enabling us to impart our feelings to others and to assess their mental state and intentions, processes known as "empathy" and "theory of mind" (ToM). Allostasis, self-reference, and ToM are proposed as special competencies for humans (Dehaene et al. 2022). The functional and anatomical architectures are yet to be fully characterized.

Very brief, lateral brain systems are mainly linked to functional integration related to extrapersonal space, such as exteroception and proprioception (Mesulam 1987). Conversely, the internal world of the embodied brain, including interoception, nociception, and its elaborations, such as selfhood and emotional inference, is primarily linked to the cortical areas located on the medial side of the hemispheres (Mesulam 1987). Initially identified by Broca as the "limbus," Papez later delineated the cortical areas linked by the cingulum and fornix as the *medial system* (Papez' circuit) and associated this system with "emotion" (Papez 1937). Subsequently, Maclean expanded this framework to include the "visceral brain" (rhinencephalon), the amygdala, and parts of prefrontal cortex (PFC) and temporal lobe, coining the term "limbic system" (MacLean 1955).

It is important to note that this lateral-medial distinction is orthogonal to the well-established anterior–posterior segregation of action selection and planning in the anterior part, the frontal lobe, versus sense-making and perception in the posterior part, comprising parietal, temporal, and occipital lobes (Goldstein 1925). However, in current understanding, cognitive functions depend on the bi-directional interaction between anterior and posterior parts (Mesulam 1987; Rizzolatti et al. 1997; Fuster 2004; Friston 2010; Kwon et al. 2025).

According to Nieuwenhuys and Puelles (Nieuwenhuys and Puelles 2016), a good brain model should consider anatomical coordinates that are consistent and unaffected by deformations, arranging units along both the anterior–posterior and dorso-ventral axes. A model adhering to this premise has recently been described for the lateral brain systems, involved in engaging with the external environment through exteroception, proprioception, and action. This domain-general dual-loop model (Weiller et al. 2022) (Fig. 1A) consists of integrating hubs within the action-oriented frontal lobe (A) and the perception-associated posterior lobes (P), interconnected via two distinct tracts, dorsal and ventral of the Sylvian fissure, corresponding to two pathways with differing computational capabilities. The hubs are the new and essential feature. Multiple parallel domain-specific loops are integrated into the hubs. The distinction between dorsal and ventral relates to the well-known formulation of a dorsal "where/how" and a ventral "what" pathway in the visual domain (Macko et al. 1982), later extended to other domains, eg the auditory (Romanski et al. 1999; Saur et al. 2008). The model elucidates how signals
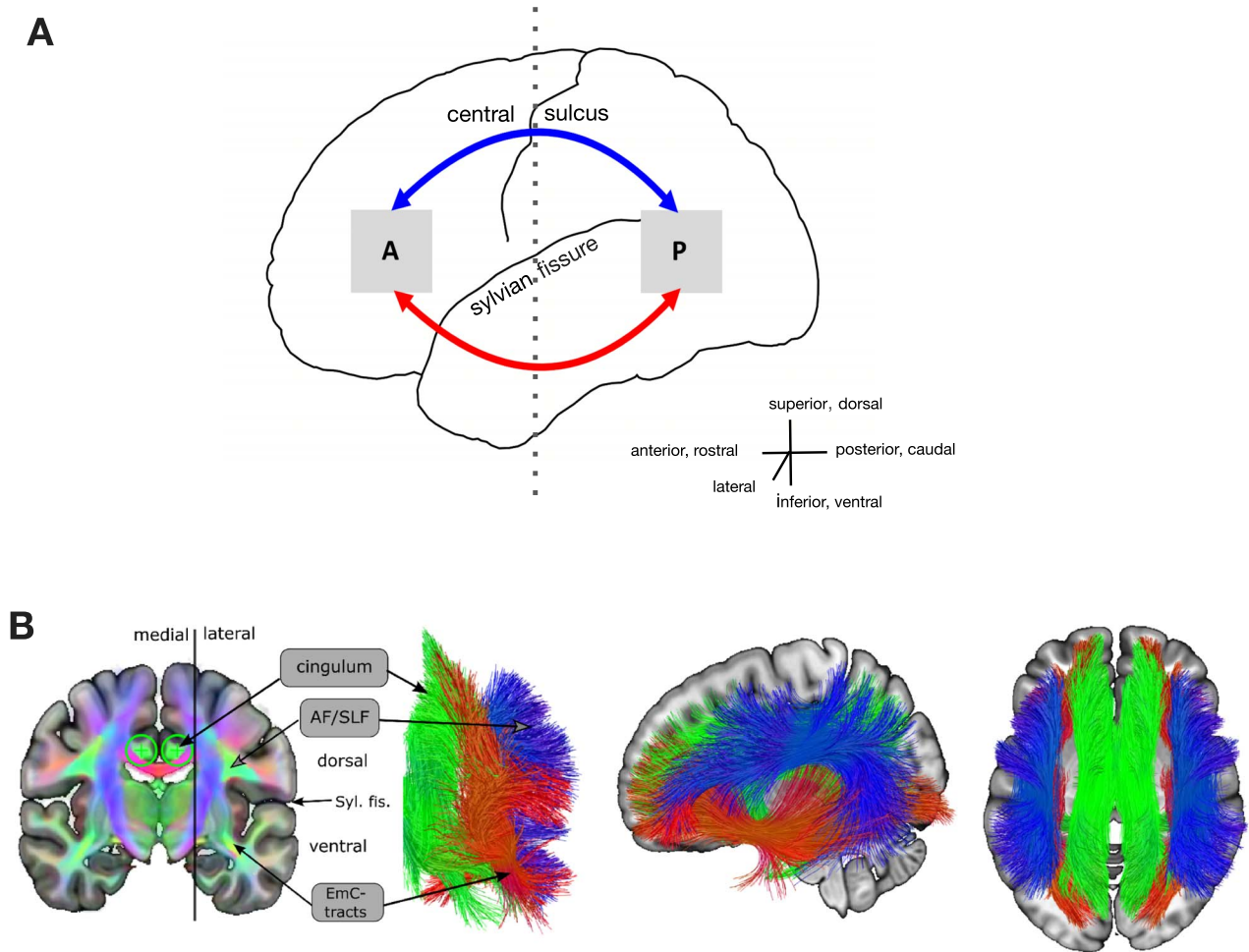
A

B

Fig 1. The dual-loop principle. A) Integrating hubs within the action-oriented frontal lobe (A) and the perception-associated posterior lobes (P) are interconnected via two distinct tracts, dorsal and ventral of the Sylvian fissure, crossing the central sulcus and corresponding to two pathways with differing computational capabilities. The dotted line indicates the approximate position of the coronal slice shown in B). B) Anterior–posterior (AP) traversals of streamlines (coded green in typical diffusion imaging RGB convention) on a coronal slice at the level of the central sulcus. The AP traversals are bottlenecks and were used to define ROIs for tract selection (Fig. S1). Three large tract systems connecting the cerebral cortex in the frontal and the posterior lobes were found (for fornix, see Fig. S2). The medial-dorsal streamlines ("cingulum") are coded green, the lateral-dorsal streamlines ("AF/SLF") are coded blue, and the ventral streamlines ("EmC") are coded red. Syl. Fis. = Sylvian fissure. Views from front, left, and above.

from the external world are understood. The presence of the two hubs allows for a closed loop, enabling internalization and thus the connection of internal representations of the external world with abstract concepts independent from the moment, fostering mind wandering, foresight, and reflection. With conversation partners, who have the same ability, we can communicate about things that are not present.

Just as we perceive and interact with the external world, we also engage with the internal world—encompassing the body, memory, and emotional experiences (Benarroch 1993). A comparable dual-loop mechanism as in the lateral system is likely to operate within the medial brain system linking appraisal processes in the medial PFC (MPFC) with biographical and episodic memory functions in the precuneus (Brodt et al. 2018; Coenen et al. 2022). Moreover, we possess the ability to connect emotions to both past and future experiences (Johnson 2025). For instance, we may feel a pang of regret when recalling a failed exam or a sense of anticipation for a long-awaited reunion. The closed-loop system facilitates internalization, enabling emotional evaluations to be made independently of the immediate context while informing self-referential processing (Lyu et al. 2023) and allowing us to envision a (preferably positive) future.

Our main question pertains to an even broader subject. Cognitive functions emerge from the interplay of widely distributed networks. Processes such as allostasis, self-reference, and ToM depend on the interaction of both medial and lateral systems. Thus, how does the brain achieve integration between these two systems?

Given that studying the brain's connections may contribute more readily to understanding its function than examining cortical parcellations (Goldstein 1925; Bullmore and Sporns 2012; Thiebaut de Schotten and Forkel 2022; Tucker and Luu 2023; Weiller and Rijntjes 2023), we here focused on association tracts which connect cortical regions within one hemisphere. There are three principles of organization to be considered for each hemisphere: lateral-medial, anterior–posterior, and dorsal-ventral. The trajectory of the central sulcus forms the anterior–posterior axis by separating the cerebral cortex into anterior (frontal lobe) and posterior (parietal, temporal, and occipital lobes) parts. The lateral (Sylvian) fissure establishes the dorso-ventral axis by dividing the cortex into dorsal (superior) and ventral (inferior) parts. To identify connections between the anterior and posterior parts of the brain, we searched for all streamlines that cross below the central sulcus. Thus, we looked at streamlines traveling

in an anterior–posterior direction (AP traversals) (green in RGB mode) at a sagittal section around the level of the central sulcus (Fig. 1B). There are four such traversals. In a previous study, we identified two of them, both lateral from the thalamus, one located superior to the Sylvian fissure (ie dorsal) and one below the Sylvian fissure (ie ventral) (Weiller et al. 2022). Now, we added the medial traversals and determined where, in the cortex, the fibers traveling through these four AP traversals converge to find the cortical hubs for cognitive functions.

Materials and methods
Participants
The data used are part of the Human Connectome Project (3T HCP; https://ida.loni.usc.edu/login.jsp). We extracted diffusion MRI (dMRI), resting-state functional magnetic resonance imaging (rsfMRI), and behavioral data from 183 participants (100 females, 83 males, mean age: 30 ± 3.9) from the HCP (Q1:S3) data corpus, which has a resolution of 1.25 mm isotropic for dMRI and 2 mm isotropic for rsfMRI.

Diffusion-weighted MRI
Each gradient table includes approximately 90 diffusion weighting directions plus $b = 0$ acquisitions interspersed throughout each run. Diffusion weighting consisted of three shells of $b = 1,000$, 2,000, and 3,000 s/mm^2 interspersed with an equivalent number of acquisitions on each shell within each run (18 $b0$, 3 shells where each shell has 90 directions). For preprocessing, see (Glasser et al. 2013). Images were spatially processed using the warps generated by the HCP pipeline. These warps transform the data into Montreal Neurological Institute (MNI) standard space. Results are displayed on an average T1 image and average surface created in VBM8 from 550 healthy participants from the IXI-database (https://brain-development.org/ixi-dataset/) and normalized into MNI standard space (ICBM152 2009b asymmetric). For anatomical nomenclature of cortical regions, we used the human brain atlas by Mai and Majtanik (Mai and Majtanik 2017) for reference. This atlas is based on a young adult brain with high consistency of slices and is widely used, combining comprehensiveness and precision and is registered to the MNI space.

Tractography was performed based on a global approach (Reisert et al. 2011; Weiller et al. 2021). Global tractography per se is neither deterministic nor probabilistic. Global tracking avoids the bias of predetermined starting and stopping points and makes the analysis free from any a priori definition of tracts. Determining aspects are introduced on the second level. In the first step, whole-brain connectomes were reconstructed based on dMRI data from each individual participant. Subsequently, regions of interest (ROIs) (see below) defined in atlas space (by MNI coordinates or explicit masks) were warped into participant space and are used to select particular bundles out of the pre-existing connectome. The tracking procedure itself hence occurs independently from the ROIs. As opposed to local walker-based tractography, global Gibbs tractography (Reisert et al. 2011) uses a random point process to generate streamlines and searches for their best alignment to the present diffusion MRI data. This approach creates a fiber configuration that delivers the best explanation for the acquired diffusion-weighted MRI data (Fillard et al. 2011). It is usually robust in terms of noise, and fiber densities are directly related to the measured data themselves (Fillard et al. 2011; Reisert et al. 2011; Schumacher et al. 2018). We followed the publicly available method proposed in (Reisert et al. 2011) and used the "dense" preset offered by

the toolbox, which automatically sets the parameters according to both the resolution and diffusion signal. This setting results in approximately 150,000 streamlines for an HCP dataset. In addition, to increase reproducibility, we increased the number of fibers using the following accumulation strategy: After the cooling-down phase, the temperature was again increased to 0.1, and the state was further iterated for 10^7 iterations. This procedure was iterated over five rounds, and the tracts resulting from each round were accumulated to obtain one final tractogram that was 5-fold larger than the initial one. This results in a tractogram of approximately 800,000 streamlines in a dataset from a single HCP volunteer. The approach was proposed by (Schumacher et al. 2018) and showed a much higher level of retest reliability. For the area of reconstruction, we used all white matter regions defined in the white-matter parcellation accompanying the HCP data corpus. The resulting white-matter mask was additionally slightly dilated further to capture the white/gray matter transition zone. After reconstruction, the specific streams or bundles were selected based on automated selection protocols (see below). To pool participant information on the group level, streamline terminal maps and streamline orientation density maps for each selected bundle were rendered on an isotropic matrix with a resolution of 1.25 mm. The densities were then warped to MNI space using the HCP-derived warping fields (onto an isotropic matrix of 2 mm) and subsequently averaged. For the streamline terminal maps, no gray-value modulation by the determinant of the Jacobian was applied. Cortical conjunction maps were rendered as the voxel-wise product of the terminal densities of the ventral and lateral respectively medial dorsal bundles, and were warped into MNI group space. For visualization, the orientationally weighted streamline densities enable simple streamline tractography to be performed on the average orientation fields to visualize the bundles on a group level, using streamline tractography as implemented in NORA (www.nora-imaging.org). Streamlines of association tracts connecting the anterior and posterior parts of the brain represent anterior–posterior traversals (green in RGB convention) on a coronal slice at the approximate level of the central sulcus (Fig. 1B). There are only four such AP traversals; two are positioned lateral from the thalamus and two medial. We used these AP traversals as ROIs on the constructed connectome (Fig. S1). The ROIs represent white matter bottleneck regions with high diffusion anisotropy containing anterior/posterior traversals. ROIs can be downloaded from: https://www.nora-imaging.org/demo/index.php?sharelink=XvSR8ufyJzb6taiqa4oTWvFzBrnKF9Wd&public.

The ventral pathway is best defined by the anterior/posterior traversal of a specific anterior/inferior part of the extreme capsule, ie lateral from the thalamus and below the Sylvian fissure. It is defined as the collection of streamlines passing through the MNI coordinates $(+/-31, 3, -10)$ with a radius of 5 mm (see Weiller et al. 2021). For the lateral dorsal pathway, we used a manually defined triangular white matter ROI (see: Weiller et al. 2022). Conceptually, the ROI was drawn in MNI space, by aligning the *xz*-plane with the central gyrus at level $y = -10$. Only those regions were included where AP traversals are present, which was determined by a color-coded fractional anisotropy (FA) map. The cingulum was selected by using a spherical ROI at MNI coordinate $(9, -12, 35)$ with a radius of 7 mm and the additional constraint that at least one tangent of the streamline within the ROI has an angle smaller than 25° with respect to the AP coordinate axis of the MNI system. This additional constraint avoids selection from transcallosal streamlines. The fornix was

defined by the simultaneous traversal of two spheres with a radius of 4 mm at MNI (0, 2, 7) and (0, −6, 14). We selected those streamlines that have at least one tangent within the ROI; these had an angle smaller than 15° with respect to the anterior/posterior MNI coordinate direction. We further restricted the selections to only contain (i) streamlines connecting the cortex and (ii) only streamlines within one hemisphere. To pool participant information at the group level, streamline terminal maps and streamline orientation density maps were rendered at the participant level (on an isotropic matrix 1.25 mm), warped to MNI space (on an isotropic matrix 2 mm), and then averaged.

rsfMRI

rsfMRI scans from each subject of the HCP corpus were preprocessed as described in Smith et al. (2013). Briefly, gradient-echo fMRI data (TR = 0.72 s, TE = 33 ms, 72 slices, multiband factor 8, 104 × 90 matrix, 2 mm isotropic resolution) were distortion- and motion-corrected, high-pass filtered with a cutoff of 2,000 s, and decomposed by spatial independent component analysis (ICA). The network components were identified semi-automatically by visual inspection after sorting them according to their correlations with the FIND atlas (Shirer et al. 2012). Artifactual components were identified by FSL-FIX and discarded, resulting in cleaned rsfMRI time series that were then averaged within each interaction hub defined from the structural streamline analysis. Functional connectivity between the hubs was then calculated as the Fisher-z-transformed correlation coefficient between the averaged time series within each hub. To measure the similarity between the investigated hubs and the resting-state networks, we took the ICA components corresponding to the most prominent networks at the group level and computed the DICE similarity measure between the group of lateral hubs and the functional network for various z-score thresholds of the ICA maps. The same was done for the group of medial hubs. The selected functional networks for this analysis are taken from the FIND atlas (Shirer et al. 2012): dorsal and ventral default mode network (DMN), Language (LAN), central executive network/executive control network (CEN), anterior and posterior salience network (SAL), dorsal attention, sensorimotor, high visual, and primary visual networks. For comparison, we also computed the DICE similarity between the hubs and the 7 networks as described by Yeo (Yeo et al. 2011).

Dendrogram calculation

Data processing was performed in MATLAB R2018a. From the preprocessed rsfMRI data, average time series were extracted for each of the hub regions (LPFC, MPFC, MTG/TPOJ, PCC, TPG, AI). For each subject, all pairwise correlation coefficients between these regions were computed. The resulting correlation matrices were then averaged over subjects. The average correlation matrix was converted into a dissimilarity matrix (dissimilarity = 1-correlation). Based on this matrix, distances between the regions in the model were computed using a "complete" distance measure where larger distances correspond to higher dissimilarities.

Correlation of structure and behavior

Is it possible to associate the structural hub strength with behavioral characteristics? To explore this, we quantified the voxel-wise sum of cortical conjunction maps corresponding to the medial-dorsal, lateral-dorsal, and ventral streamlines as an index of hub strength. Pearson correlation coefficients were calculated to evaluate the relationships between behavioral measures and hub strength. The HCP dataset includes 814 behavioral measures https://wiki.humanconnecto me.org/docs/HCP-YA%20Data%20Dictionary-%20Updated%20for %20the%201200%20Subject%20Release.html). The behavioral measures within the HCP corpus are derived from a consensus-building process and include the National Institutes of Health (NIH) Toolbox, supplemented by additional assessments of visual processing, "personality and adaptive function," "delay discounting," "fluid intelligence," and emotion processing. Our experimental approach—linking anatomical conjunction strength to behavior—has not been studied before; thus, an exploratory approach was required. However, in our study's results based on anatomy, we identified cortical areas exhibiting a high conjunction strength of association tracts, which coincide with hub regions of the brain in functional networks, particularly the DMN. We used the cognitive correlates of these neural hubs from the literature to narrow the behavioral items from the HCP corpus to be investigated. The integration of internal and external worlds within the brain is inherently linked to decoupled states such as mind wandering and ToM. These characteristics have been associated with hub regions of the brain in functional networks, particularly the DMN (Mason et al. 2007; Spreng and Grady 2010; Schurz et al. 2014; Menon 2023). The DMN has also been linked to mood fluctuations and attentional problems (Raichle 2015; Broulidakis et al. 2022). Consequently, items related to social tasks, as well as those associated with emotion and affect, were considered particularly pertinent. Building upon our earlier work on the lateral dual-loop model, we hypothesized that cognitive and language-related functions might also be implicated. Since the hubs correspond to rsfMRI network nodes of the DMN, the fronto-parietal/executive network, the salience network, and the language network (as evidenced in our results), we anticipated correlations across the domains of "cognition," "emotion/affect," "social tasks," and self-ratings derived from the ASR and DSM measures. We excluded variables from the domains of "subject information," "study completion," "MR and MEG sessions," "eye-tracker meta data," "Freesurfer," "Health and Family History" (eg blood pressure, weight), "substance use," "Motor," "Sensory," "Alertness," and "Personality." Where age-adjusted versions of variables were available, we selected these and excluded their nonage-adjusted counterparts. We omitted *CogEarlyComp_ageAdj* since our cohort consisted exclusively of adults, with no children included. For the social task, we selected only the percentage (Perc) variables. Regarding self-report scales, we exclusively retained the corresponding *T*-scores, excluding *ASR_Totp_T* as it merely reflects the aggregate score across all scales. This process resulted in the selection of 41 variables for analysis. We used the entire available behavioral data set from the HCP corpus (532F, 466M, age: 28,7 ± 3.7 years). To account for multiple comparisons, we applied a significance threshold for a 5% false discovery rate, following the Benjamini–Hochberg procedure (Benjamini and Hochberg 1995), as well as the more conservative Bonferroni correction threshold.

Results

Three association tract systems link the frontal lobe to the posterior lobes.

The AP traversals on the coronal slice at the level of the central sulcus represent bottlenecks from which the streamlines expand like a butterfly: two medio-dorsal ROIs above and below the callosum resulted in streamlines (Fig. 1B, Fig. S2, Table S1) corresponding to the cingulum (denoting the fibers, not the cingulate cortex) and fornix. One lateral-dorsal ROI captured a streamlined convolute corresponding to the arcuate fascicle

(AF) and superior longitudinal fascicles (SLFs). One ventral ROI captured a streamline convolute in the extreme capsule (EmC) comprising the uncinate fascicle (UF), the temporo-frontal extreme capsule fascicle (TFecF), and the inferior fronto-orbital fascicle (IFOF) (Weiller et al. 2021).

Lateral and medial dual loops

Global tracking allows extending streamlines to cortical regions in the trajectory of the last part of the fibers, resulting in cortical termination maps (Weiller et al. 2021). The cortical termination maps of the lateral dorsal (AF/SLF) and the ventral system (EmC) are described in the dual-loop model (Weiller et al. 2022). The fornix streamlines connect subcortical structures, cerebellum, brainstem, and allo- and periallocortex (Table S1). The cingulum cortical termination maps comprise most of the medial wall of the hemispheres (areas 7 to 11, 23 to 26, 29 to 33) (Table S1).

To assess the joint cortical terminations as the anatomical sites for interaction of the medio-dorsal, the lateral-dorsal, and ventral tract systems defined above, we performed a pairwise conjugation of streamlines by multiplying the corresponding cortical probability densities on the cortical surface (Weiller et al. 2022). The medio-dorsal and lateral-dorsal streamlines did not conjugate with each other. However, both dorsal streamlines conjugated separately with the ventral streamlines (Fig. 2A, Table S2). The lateral-dorsal streamlines (AF, SLF) conjugated with the ventral streamlines (EmC) in a hub in the frontal lobe, in the lateral PFC (LPFC:anterior middle frontal gyrus (aMFG) [area 46], inferior frontal gyrus (IFG) [area 45A, 47/12,44]) as well as in a hub in the posterior lobes ("MTG/TPOJ") comprising the middle temporal gyrus (MTG) and temporo-parietal-occipital junction (TPOJ) (Fig. 2B and C). A further hub was found in the anterior insula (AI). These are the known hubs of the lateral dual-loop model (Weiller et al. 2022).

The conjunction of the medio-dorsal streamlines (cingulum-/fornix) with the ventral streamlines (EmC) resulted also in two hubs, one in the frontal lobe and one in the posterior lobes. The frontal lobe hub comprised the MPFC (anterior cingulate cortex [area 24], prelimbic cortex [area 32], infralimbic cortex [area 25] and granular areas 9 and 10 [see: Passingham 2021]), extending to orbital PFC (oPFC) (medial, central, and lateral oPFC (areas 14/11/13/orbital surface of 47/12). The posterior hub was in the posteromedial parietal lobe with a large cluster in the precuneus (posterior cingulate cortex [PCC]) and retrosplenial limbic gyri (von Economo) (areas 23, 31, 30), extending into the parahippocampal region, amygdala, and a large cluster in the temporopolar gyrus (TPG, area 38). Not all streamlines of the three convolutes were part of conjugation hubs: only cingulum streamlines conjugated with ventral streamlines, not the fornix streamlines. Nonhub lateral-dorsal streamlines project to what is termed secondary or unimodal association cortex (Mesulam 1987). Ventral streamlines that do not participate in the hubs were found in parts of anterior and inferior frontal lobe, in the anterior and inferior temporal lobes and in the posterior occipital lobe, as described previously (Weiller et al. 2022). For the purpose of this study, only streamlines that projected on the hubs were considered further. Defined by the four hubs two separate circles along dorsal and ventral pathways with interaction hubs in frontal and posterior lobes are formed. The lateral circle corresponds to the lateral dual-loop model, the medial circuit constitutes a medial dual loop.

Functional and anatomical connectivity reveal a meta-loop

rsfMRI data from the same HCP participants were employed to explore the functional connectivity of the anatomically defined hubs. We used the functional connectivity between the six anatomical hub regions as input for hierarchical agglomerative cluster analysis of functional connectivity strengths (Fig. 3A, Fig. S3). The dendrogram, for each hemisphere, displays two strongly correlated functional fronto-posterior pairs. One functional pair corresponds to the anatomical conjunction of ventral streamlines with lateral-dorsal streamlines in the LPFC and MTG/TPOJ, forming the lateral dual loop. The other functional pair reflects the conjunction of ventral with medio-dorsal streamlines in the MPFC and PCC, constituting the medial dual loop. On the next level, these two pairs of lateral and medial hubs are merged into a supercluster, a meta-loop that combines the two dual loops. TPG and AI exhibit more heterogenous connectivity patterns. Thus, a functional meta-loop combines the four major hubs of two separate dual loops.

How does the meta-loop integrate the two dual loops, and what are the corresponding anatomical connections between the lateral dual loop and the medial dual loop? To investigate the anatomical connectivity of the meta-loop, we used the hubs of the two pairs with the strongest functional interaction (LPFC and MTG/TPOJ; MPFC and PCC) as ROIs to constrain global tracking. As depicted in Fig. 2, there were anterior–posterior connections within the two dual loops. Specifically, the LPFC is connected to the MTG/TPOJ via streamlines traversing the extreme capsule (ventral pathway) and the arcuate fasciculus/superior longitudinal fasciculus (dorsal pathway). Similarly, the MPFC is connected to the PCC via the cingulum and the ventral pathway. We found few diagonal longitudinal anterior–posterior connections between medial and lateral hubs along the ventral pathway (MLPF-MTG/TPOJ and LPFC-PCC). However, they could be artifacts created by intermingling fibers in the extreme capsule (Weiller et al. 2021). Furthermore, the long distance between the first and the second subtree in the dendrogram does not favor functional diagonal connections.

Clear anatomical connections were found between the two frontal and the two posterior hubs (Fig. 3B). The streamlines connecting the frontal hubs, LPFC, and MPFC correspond to the frontal short association tract (fsat) (Oishi et al. 2008), while those connecting both posterior hubs PCC and MTG/TPOJ align with those belonging to the middle longitudinal fascicle (MdLF) (Schmahmann and Pandya 2006; Makris et al. 2017). Thus, the meta-loop is capable of functionally integrating both dual loops through anatomical anterior and posterior cross-connections between the hubs.

The cognitive intrinsic functional networks map onto the anatomical hubs

To frame the hubs functionally, we compared the anatomically defined hubs with the established functional networks using classical independent component analysis of the rsfMRI data from the same participants. The independent component analysis separates the low-frequency fluctuations of the blood-oxygen-level-dependent (BOLD) signal into spatially independent maps with common time courses. Interpretation of the resting-state spatial maps is based on comparison with known patterns of task-dependent activation or deactivation; for this purpose, we used the FIND atlas (see Materials and Methods). There are approximately 10 to 11 networks that consistently appear in rsfMRI (Damoiseaux et al. 2006), whereby the ICA may break down single functionally defined networks into separate subnetworks (for instance, the DMN is broken down into "dorsal" and "ventral" DMN). The networks related to primary functions (sensory, motor, vision) and visuospatial processing did not relate strongly to the anatomical hubs. However, the nodes of the networks related
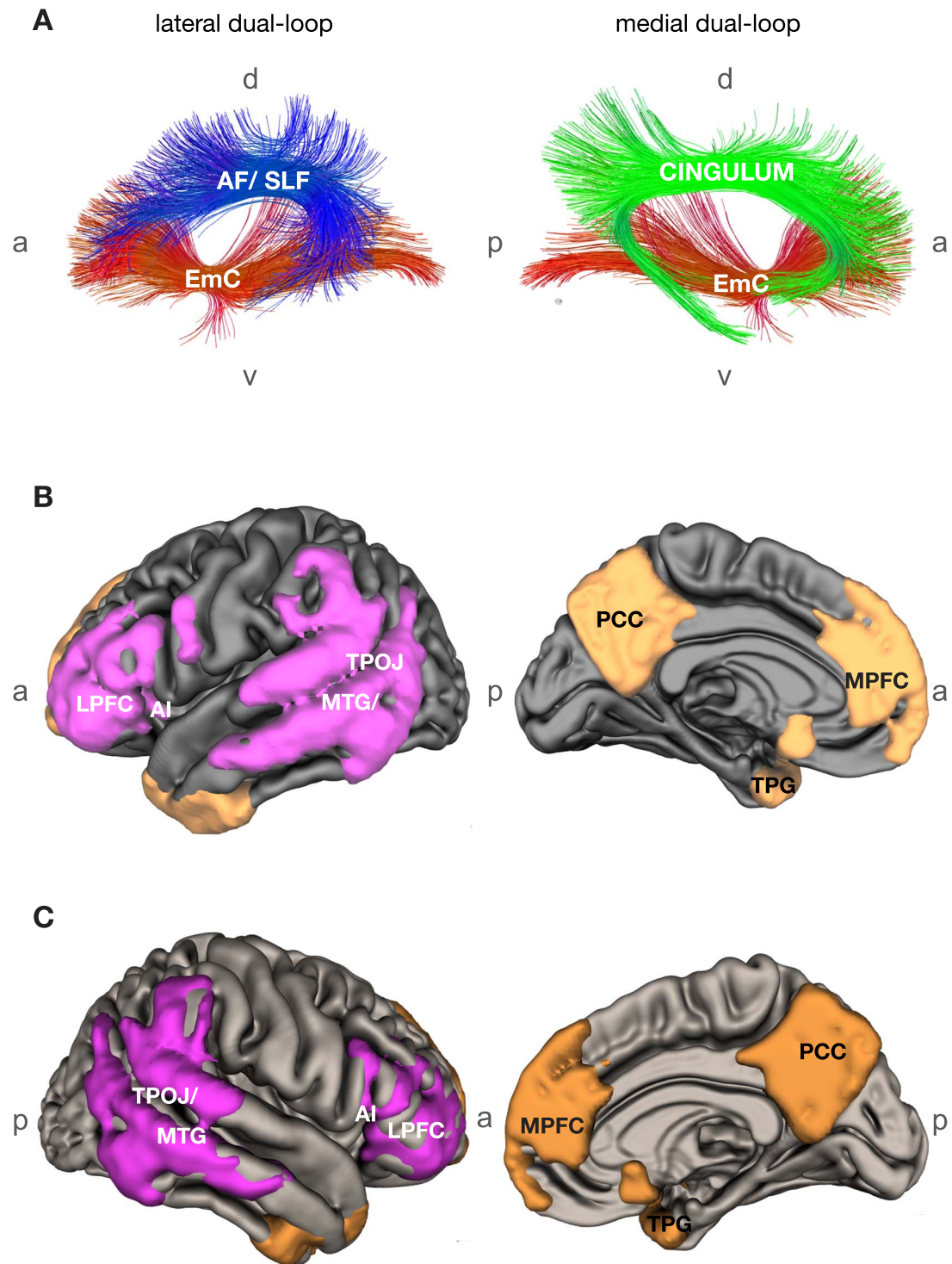
Fig. 2. Anatomical interaction sites ("hubs") between the ventral and the two dorsal systems. The left column presents a lateral view, while the right column displays a medial view. A) Two dual loops: the lateral dorsal streamline systems (AF/SLF) and the separate medial dorsal streamline system (cingulum) each form a dual loop with the ventral streamline system (EmC) to connect frontal and posterior lobes; d = dorsal, v = ventral, a = anterior, p = posterior. B, C) The hubs as the voxel-wise product of the permutation of dorsal and ventral streamlines: Ventral × medial-dorsal conjunction (ochre) was in the medial prefrontal cortex (MPFC), posterior cingulate cortex (PCC), and temporopolar gyrus (TPG). Conjunction of ventral × lateral-dorsal (magenta) was in the lateral prefrontal cortex (LPFC), anterior insula (AI), and in a large posterior cluster centered on the middle temporal gyrus (MTG) and temporoparietooccipital junction (MTG/TPOJ). B) Left hemisphere and C) right hemisphere.

to higher cognitive functions, the DMN (Raichle 2015), the CEN, also called the fronto-parietal network or multiple demand network (Duncan 2010; Yeo et al. 2011; Chand et al. 2017), the SAL (Seeley 2019), and the language network participate in all four anatomical conjunction hubs (Fig. 4; Table S2). For quantification,

we computed the DICE scores between the ROIs of the FIND atlas and the group of lateral and medial hubs (Fig. S4). The quantitative analyses corroborate the visual impression. The similarity between the anatomical hubs and the DMN is most obvious for the medial system (PCC and MPFC) (Fig. S4) and
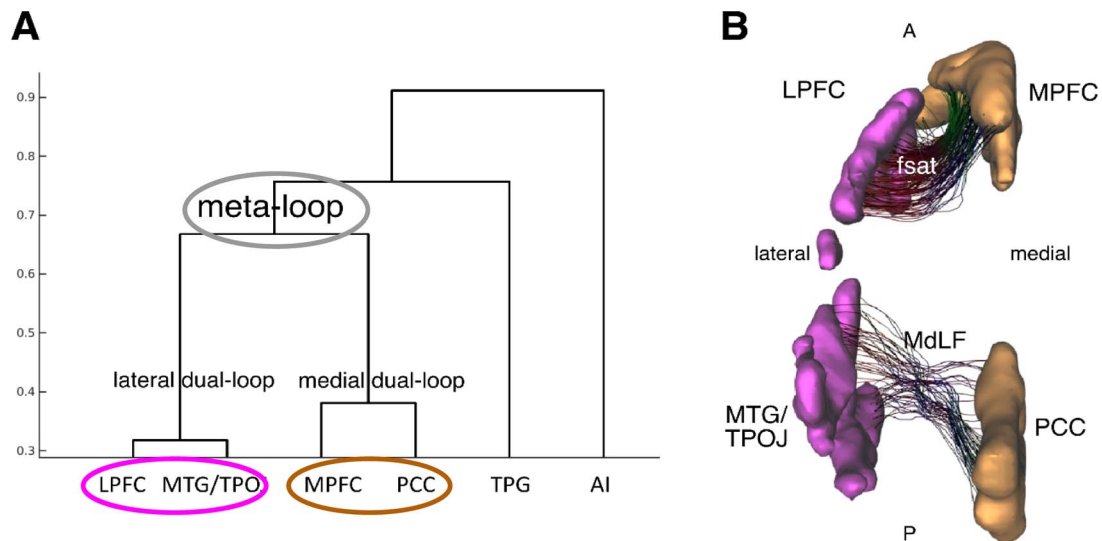
Fig. 3. Structure of the meta-loop. A) Dendrogram of functional connectivity strengths validates the classification in two dual loops, which are merged into a supercluster on the next level. B) The separate hubs of both dual-loops are connected along cross connections (left hemisphere shown; A = anterior, P = posterior); anterior–posterior connections within the lateral and the medial dual-loop are omitted for clarity.

inferior parietal lobe (MTG/TPOJ). But also, vPFC as part of the LPFC cluster is a typical DMN node (Raichle 2015). It has been discussed whether the entorhinal cortex and TPG are also part of DMN (Raichle 2015). In the lateral system, the large cluster in the LPFC relates best to the major node of the executive control network (CEN) (Duncan 2010) (middle frontal gyrus) and to the language network (inferior frontal gyrus) (Binder et al. 2009). The AI is clearly an anatomical interaction hub and central to the functional SAL (Seeley 2019). We repeated the analysis using the seven networks as originally defined by Yeo et al. (Yeo et al. 2011) and observed very similar results (Fig. S4). The medial dual loop predominantly corresponds to the DMN, while the lateral dual loop is primarily associated with the frontoparietal network.

Individual anatomical conjunction strength correlates with performance in ToM tasks

Behavioral scores from the HCP dataset can be used for correlation with structural connectivity data in individuals. For this purpose, the number of conjugated streamlines between the three tract systems were taken as a measure of "hub strength." Out of the 814 behavioral items in the HCP dataset, we tested 41 that have been related to cognition, emotion/mood, and the social task. Only ToM measures from the social task correlated with "hub strength" on an "individual level" in both dual loops. On a lower significance level, a correlation was found between hub strength in the lateral dual loop and verbal reasoning, general verbal vocabulary knowledge, and reading skills (more on the left side), as well as attention and attentional problems, externalization, and withdrawal or avoidance behavior (Table S3).

Discussion
Hubs as interaction sites for two dual loops

Unlike the current trend of ever finer differentiation of the cerebral cortex, we divide the brain based on the two most invariant structures on a macroscopic level, the central sulcus and the Sylvian fissure (Mesulam 1987). The nearly vertical central sulcus divides the hemisphere into front (anterior, rostral) and back (posterior, caudal), while the more horizontal Sylvian fissure

divides the hemisphere into top (superior, dorsal) and bottom (inferior, ventral) (Fig. 1A, Fig. S1). Only three long association tract systems, following either a dorsal or ventral course, connect the cortex of the frontal and posterior lobes. Streamlines of the three tracts converge in two sets of anatomical "hubs." One set is part of the lateral brain systems, which are more concerned with extrapersonal space (eg exteroception and proprioception), while the other set belongs to the medial brain systems, specialized in processing the internal world of the embodied brain.

The three tracts can be used to order the cerebral cortex, corresponding to established serial models of the cortex (Fig. 5A). These approaches are data-driven, focusing on patterns formed by cortical regions sharing common characteristics based on architecture at cellular, molecular, geometrical, and circuit levels and incorporating onto- and phylogenetic developments (Mesulam 1987; Park and Friston 2013; Margulies et al. 2016; Amunts et al. 2020; Luppi et al. 2022; Pang et al. 2023; Tucker and Luu 2023; Du et al. 2024). Primary cortex regions (V1, A1, S1, M1) are not targeted by the three tracts. We used single ROIs to define the streamlines of the three systems (Fig. S1). Therefore, we did not differentiate separable subtracts, for instance, AF and SLF that together constitute the dorsal pathway (Weiller et al. 2022; van den Hoven et al. 2024), nor IFOF, UF, and TFecF, which constitute the ventral pathway (Weiller et al. 2021), nor subdivisions of the cingulum bundle (Jones et al. 2013).

However, our approach enables a classification of the association cortex into nonhub and hub regions. Nonhub regions are exclusively connected via either medial or lateral dorsal streamlines or through ventral streamlines. The nonhub regions within the lateral system are associated with the unimodal association cortex (eulaminate III) located adjacent to, and interconnected with, primary cortical regions (Mesulam 1987). This type of association cortex is connected via dorsal streamlines that do not integrate with the ventral system, such as the "dorso-dorsal pathway" between the superior parietal lobule and the dorsal premotor cortex (Sakreida et al. 2016). Similarly, nonhub ventral streamlines connect to the orbitofrontal, inferior temporal, and occipital lobe (Weiller et al. 2022). In the medial system, all fornix streamlines are independent of ventral streamlines. The fornix connects
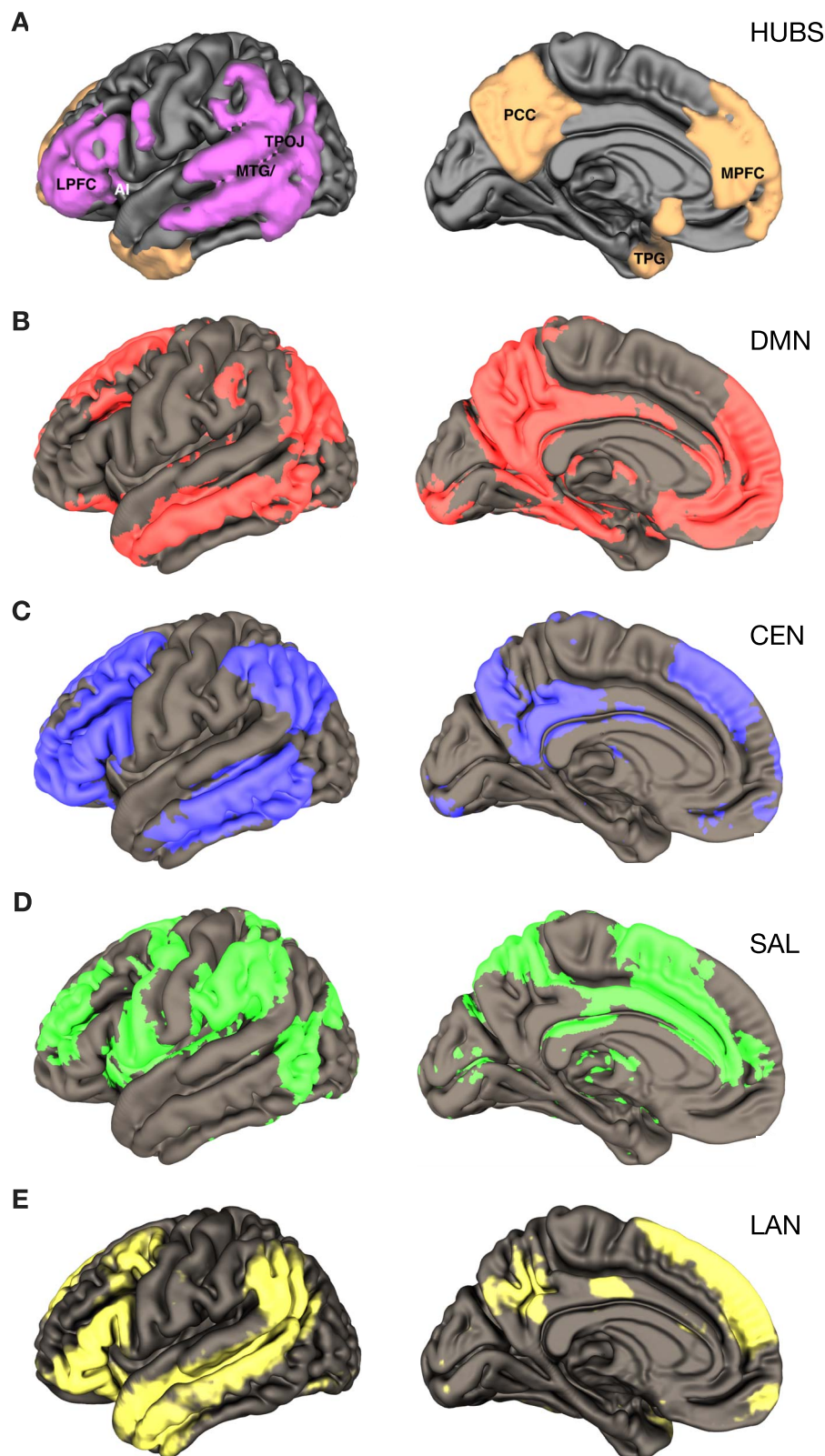
Fig. 4. A–D) The cognitive functional networks of the brain derived from resting-state network analysis that project on the anatomical hubs (left hemisphere): A) the anatomical hubs, B) the default mode network (DMN), C) the central executive network (CEN), D) the salience (SAL) network, and E) the language network (LAN).

the allocortex and periallocortex, forming the inner limbic arc (Mesulam 1987; Puelles et al. 2019).

The fornix functions as a fast and automatic loop, relaying stimuli from the viscera, as well as olfactory, auditory, and visual stimuli (via the colliculi) to the hypothalamus and mammillary bodies (postcommissural fornix) to regulate organ functions critical for maintaining the body's homeostatic integrity (Benarroch 1993). Additionally, it facilitates the transfer of episodic memory
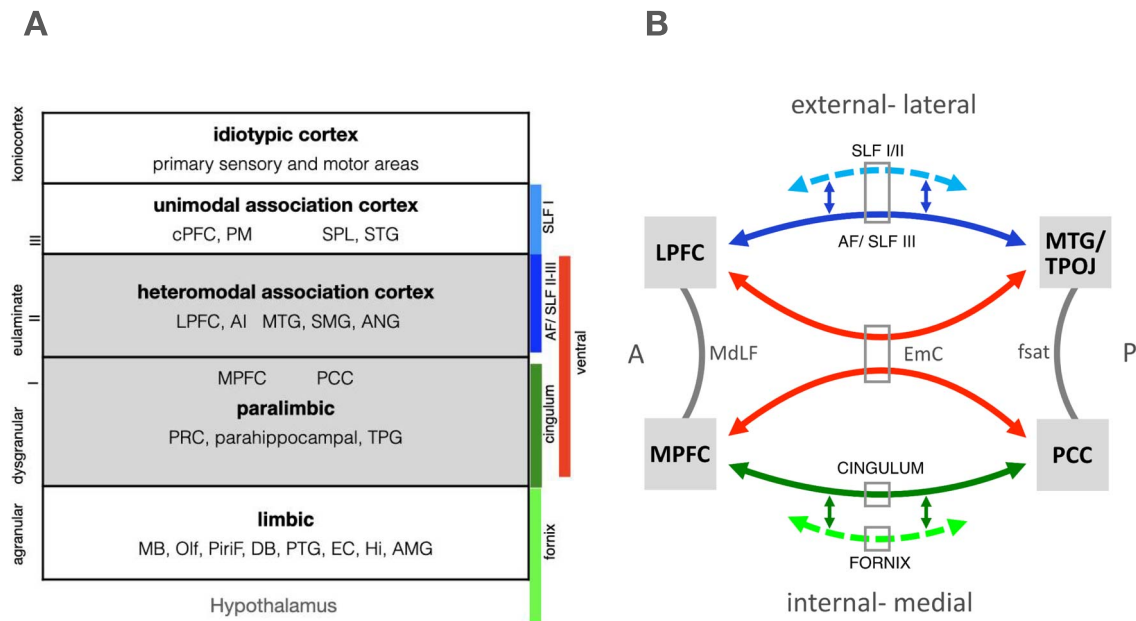
A

B

Fig. 5. A tract-based model of the brain. A) The diagram relates cytoarchitectonic features (left) to cortical terminations of the long association tracts (right) along a modification of a classic serial diagram by Marcel Mesulam (Mesulam 1987), hub regions in gray. Abbreviations of anatomical structures according to Mai and Majtanik (2017). B) The integrative meta-loop model (left hemisphere shown only), A: anterior; P: posterior; fsat: frontal short association tract; MdLF: middle longitudinal fascicle; ROIs for streamline selection as gray quadrangles.

information between parts of the hippocampal formation and mammillary bodies (Rolls 2015).

In contrast, we define hub regions as those connected by both dorsal (medial or lateral) and ventral streamlines. The hubs of the lateral dual loop, serving as cortical interaction sites for the ventral and latero-dorsal tracts (LPFC, MTG/TPOJ), correspond to the heteromodal association cortex (eulaminate I/II). Within the medial system, only the cingulum integrates with the ventral streamlines. The hub regions of the medial system consist of agranular and dysgranular proisocortices, forming the "meso-cortical ring" in the prosomeric model (Puelles et al. 2019). Our findings align with the established structural model of the brain, which posits that similar cytoarchitectonic areas are reciprocally connected (García-Cabezas et al. 2019) (Fig. 5A).

The existence of such long-distance connections has been confirmed in primates and in part by human in vivo studies (Petrides and Pandya 2012) (for a detailed description of the connections of the medial regions see supplementary text, for the lateral regions, see: Weiller et al. 2022). In our data, the lateral-dorsal and medio-dorsal streamlines are clearly separated. This division reflects their ontogenetic origins. The viscera, associated with the medial system (MacLean 1955), arise from the endodermal germ layer, whereas the tactile, visual, and auditory receptors, which mediate interaction with the extrapersonal world and are represented within the lateral system, develop from the ectodermal germ layer (Brodal 2004). The separation of the medial-dorsal and the lateral-dorsal loop is also congruent with the brain's arterial supply. The medial hubs are in the territory of the anterior cerebral artery, while the lateral hubs are in the middle cerebral artery territory.

"Hubs" are commonly defined as brain regions that participate in multiple networks, thus being highly interconnected with other brain regions and involved in linking segregated processing streams and networks, thereby playing a central role in cognitive processes. Our approach matches these assumptions. The objective was to identify anatomically the hubs that facilitate integration between the frontal and posterior lobes. However,

these hubs are not merely points of conjunction for the long association fibers linking the frontal and posterior lobes; they also represent high-level multimodal areas, integrating information for instance within the frontal lobe itself. The LPFC is extensively connected to numerous regions within the frontal cortex (Petrides and Pandya 2012; Passingham 2021). Within the hub in the LPFC, "domain-general" and "domain-specific" circuits are interdigitated (Assem et al. 2025). Rather than the frontal pole, it is the anterior portion of the middle frontal gyrus and the anterior segment of the IFG that are considered the hierarchical apex of frontal control (Passingham 2021). When Jones and Powell conducted research to find evidence of integration across all three sensory modalities (somatosensory, visual, and auditory) in primates, they identified "areas of convergence" in regions corresponding to the hub areas identified in this study. These include the posterior two-thirds of the superior temporal sulcus—which partly corresponds to the MTG in humans—and the LPFC beneath the arcuate sulcus (areas 45 and 47) (Jones and Powell 1970).

The conjunction of long association tracts identifies cortical regions with high conjunction strength, which are known in the literature from studies using very different approaches as for instance rsfMRI. The anatomically defined hubs are very similar to the nodes of functional networks, the DMN (Raichle 2015), the CEN, also called the fronto-parietal network (Yeo et al. 2011) or multiple demand network (Duncan 2010; Chand et al. 2017), the language network, and the SAL (Seeley 2019). The DMN, the SAL, and the CEN have been grouped as "core cognitive networks" in the triple network model (Menon 2011). The SAL is thought to mediate switching between internal (DMN) and external (CEN) cognitive functions. The hubs are also the place for interaction between the three networks. Highly cognitive processes are believed to be described by these three core cognitive functional networks, and disruptions are closely associated with cognitive impairments (Chand et al. 2017; Ereira et al. 2024). The language network is strikingly similar to the DMN; semantic processing constitutes a large component of the cognitive activity occurring during "passive" states (Binder et al. 2009; Dehghani et al.
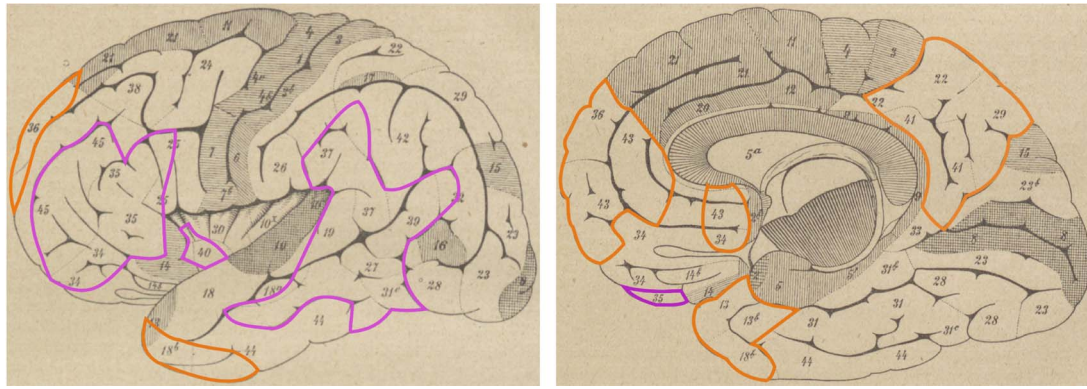
Fig 6. The anatomical hubs (magenta for the lateral dual-loop (left) and ochre for the medial dual loop (right)) correspond to the fields that are the latest to be myelinated on the Flechsig map from 1920. The range is from 1 (earliest) to 45 (latest). The hubs correspond to the fields 39–45. Copyright for the original figure at: Universitätsbibliothek Freiburg i.Br./Historische Sammlungen (V9069, b), with permission.

2017). The behavioral variables correlating with the anatomical conjunction strength in the hubs (Table S3) have consistently been associated with these functional networks. ToM is typically linked to the DMN (Spreng and Grady 2010; Schurz et al. 2014; Menon 2023), but the DMN has also been associated with crystallized abilities and reading (Geranmayeh et al. 2016; Lombardo and Kaufmann 2023), externalization (Lee et al. 2024), withdrawal (Saris et al. 2020), avoidance (Sayalı and Badre 2019), and attention-deficit/hyperactivity disorder (Broulidakis et al. 2022). Functional connectivity denotes temporal correlations between remote neurophysiological events for which the causal relation (ie the anatomical connections) is undetermined (Yeo et al. 2011). The interaction of the three association tract systems provides the common anatomical scaffold of these networks, the factual cause (Deco et al. 2011). Although the terms DMN, CEN, and SAL refer to distinct functions and the functional networks engage lateral and medial anatomical brain systems to varying extents, the DMN being more associated with the medial system and the CEN/FPN with the lateral system (Fig. S4), they all necessitate the interaction of both systems, being fundamentally based on the interplay between the internal and external worlds. A study of independent architectural gradients in rsfMRI data, contrasting between processing information from the external environment and the internal milieu resulted in the same four anatomical hubs as the first of three gradients (Zhang et al. 2019).

The hubs are the brain regions that developed the latest, ontogenetically as well as phylogenetically (Hill et al. 2010; Schwartz et al. 2023). This is illustrated when comparing the hub regions with the timepoint of myelination in an individual's lifespan as assessed by Paul Flechsig (Fig. 6) (Flechsig 1920). The range is from 1 (earliest) to 45 (latest). The hubs correspond to the fields 39 to 45. These fields myelinate as late as at the age of 25. The hubs are not only the latest in development, but they are also the first and most severely affected cortical regions in Alzheimer's disease (Jagust and Mormino 2011; Benzinger et al. 2013). It appears that these regions are vulnerable to ß-amyloid deposition as they rely on aerobic glycolysis for rapid generation of adenosine-5′-triphosphate (Jagust and Mormino 2011). We do not present data from patients with Alzheimer's disease; however, a recent study showed that altered connectivity between parahippocampal formations and the hubs in MPFC and TPOJ predict future dementia incidence (Ereira et al. 2024). It may seem promising to study structural conjunction strength in such cohorts as well.

Along a principal gradient of macroscale cortical organization, the regions of our "hubs" are described as the top of the functional hierarchy (Margulies et al. 2016), "supra-areal association megaclusters" (Du et al. 2024). They show high functional connectivity in humans (Buckner et al. 2009) and constitute the high-cost components of networks (Bullmore and Sporns 2012; Castrillon et al. 2023), the "synergistic core for human brain evolution and cognition" (Luppi et al. 2022). They reflect the high frequency/short wavelength mode of cortical activity constrained with geometric eigenmodes (Pang et al. 2023). Our data provide the structural anatomic basis. All of these models put the cortical regions that we found as conjunction hubs in an intermediate position between the limbic allocortex and the fully developed isocortex of the primary cortex, regions providing neural bridges that mediate between the internal and the extrapersonal world (Mesulam 1987).

Interaction in the meta-loop: four principles of brain organization

Looking at the connections provides structure. Starting from AP traversals at the level of the central sulcus, we identified three fronto-posterior tract systems, two dorsal, thus above the Sylvian fissure and one ventral below the Sylvian fissure, that group into a lateral and medial dual loop with respective conjugation hubs in frontal and posterior lobes. The two dual loops are anatomically and functionally separated but interact through frontal and posterior cross connections forming a meta-loop on a higher level (Fig. 5B). With respect to lateralization of higher brain functions, functionally different connotations for left and right "meta-loops" can be expected, and the interplay between the two may pose yet another level of organization. However, these questions are beyond the scope of this study. In the future, the anatomical meta-loop as described here needs to be put into context to subcortical structures of emotion regulation and the basal ganglia; the brainstem and their conjunctions with cortico-petal mostly frontal connections have to be included (Coenen et al. 2022). There is also a need to implement other anatomical networks within the frontal or the posterior lobes, thus connected by tracts that do not cross the central sulcus. Exemplary temporo-parietal cortico-cortical connections along the MdLF (Makris et al. 2017), lateral premotor, motor cingulate, and pre-supplementary motor area (SMA) connections to IFG along the FAT (Catani et al. 2013) or amygdala to prefrontal/orbitofrontal connections (Bracht et al. 2009) may be put forward.

The anatomical structure of the meta-loop accommodates four core architectural principles of the brain, (i) the integration of action-related activity in the frontal lobe with perception-related activity in the posterior lobes, (ii) the integration of distinct processing streams (dorsal and ventral), (iii) self-containment

for internalization, and (iv) the integration of representations of internal and external world in medial and lateral brain systems (Fig. 5B).

The first principle pertains to the location of the hubs within the anterior and posterior segments of the hemisphere. The reciprocal interaction between action and perception is indispensable for state estimation, decision-making, action selection, and planning through the combination of perceptual and active inference (Friston 2010), and a recent high-resolution neuroimaging study suggests that also "recognition" necessitates the integration of frontal and posterior activation (Kwon et al. 2025). The anatomical structures for these integrations is provided by the hubs of the lateral and medial brain systems, as demonstrated in our study. The stratified architecture of the meta-loop facilitates a hierarchical system of iterative prediction. The complete internal representation, with anterior-action and posterior-perceptive hubs, establishes an independent system to incorporate concepts as "latent" or "hidden states" (Mitchell 2021).

The second principle pertains to the interplay between two distinct circuits within the hubs: the dorsal and ventral loops. By "loop," we refer to the bi-directional connectivity between the action-oriented frontal lobe and the perception-oriented posterior lobes. The integration of the dorsal pathway with the ventral pathway establishes two critical hubs—one located in the frontal lobe and the other in the posterior lobe. These hubs represent a novel and indispensable feature of the dual-loop model (Weiller et al. 2022). The existence of hubs in both the posterior and frontal lobes is essential for the formation of a closed loop (as elaborated in the third principle) and contingent upon the ventral pathway extending into the frontal lobe, as proposed in the original framework (Macko et al. 1982; Ungerleider et al. 1989). This is a crucial difference with some current concepts suggesting a termination of the ventral pathway in the anterior temporal lobe (see for instance: (Sheth and Young 2016).

Each loop possesses unique specialized capabilities. The lateral dorsal loop is required for all exchange with the external world. Through our senses, we perceive the extrapersonal space in sequences (visuo- spatial, auditory, shapes), and our actions are executed via the sequential activation of various muscle groups. The dorsal loop is specialized for processing sequences in space ("where") and time ("when"), which informs both perception and action ("how to do") (Kravitz et al. 2013; Rauschecker 2018). This includes the fast transition and timing when one item prompts the subsequent one in the series for fluid behaviors such as reaching movements or articulate speech (Kristensen et al. 2013; Sakreida et al. 2016). Furthermore, the dorsal loop facilitates the intermediate and longer-term storage and retrieval of sequences, serving as affordances or blueprints for routine sequential activities like tool use, signing or forming chunks of information, as well as maintaining spatial constancy (Rijntjes et al. 1999; Medendorp 2011; Sakreida et al. 2016; Blumenthal-Dramé et al. 2017). Understanding these sequences is not necessary for their utilization, though they are not devoid of content. A sequence, whether heard or read and well-acquainted, is easily recognized within the dorsal loop, requiring merely familiarity with the sequence (experiential or ordinal knowledge, "skills"). Utilizing routines is cost-efficient, aligning with the brain's overarching objective to minimize surprises (Friston 2010).

Conversely, when faced with a novel sequence or an unfamiliar situation lacking retrievable specifications, the brain resorts to analogy for conceptual abstraction (Mitchell 2021) within the ventral loop (Corbetta and Shulman 2002; Weiller et al. 2022). Meaning is established by analogy (Gentner 1983; Hofstadter

and Sander 2013). Understanding requires classification and we can only classify the unfamiliar in terms of the familiar (Skinner cited by Weiller et al. 2022). Perceptual representations in the temporal lobe capture a stable configuration of information, which is utilized for categorization and recognition (Martin et al. 1996). The primary function of the frontal hub, situated in the LPFC, specifically areas 45A and 47, is to facilitate comparisons (Freedman et al. 2001; Passingham 2021). In collaboration with the dorsal loop, this mechanism supports the selection of sequences. In conjunction with the ventral loop, it serves to compare and relate items or the relationships between items based on structure, independent of their sequential position (Freedman et al. 2001; Klauer et al. 2002; Passingham 2021). Ordering a sequence not only involves piecing together individual elements step by step in the dorsal loop but also leveraging the ventral loop for a comprehensive overview of the entire series, classifying categories by identifying analogies.

Within the dual-loop model, the hubs serve to integrate processing of sequences and structure. The synthesis of sequence and structure echoes the original connotation of the ancient Greek terms "syn" (together) and "taxis" (order). This is why the dual-loop model is suggested as the neural substrate of hierarchically structured concatenation in all cognitive domains (Weiller et al. 2022). Our findings align with Dehaene's theory that the "language of thought" in humans has evolved across various domains through multiple parallel brain circuits (linguistic, musical, mathematical, spatial action, etc.) (Dehaene et al. 2022). There is indeed not one single stream for multiple cognitive contents, but there are multiple parallel streams tailored to the domain. With increasing complexity, the various dorsal streams are progressively engaged (Dehaene et al. 2022). Nonetheless, our data also do not refute the notion of a human multidomain capacity and proclivity to infer tree structures from strings (Fitch 2014). All these multiple parallel streams converge within the hub regions. This amalgamation of sequence analysis in the dorsal loop with structural analogy in the ventral loop facilitates flexible categorization, concept formation, abstraction, generalization, and counterfactual inference from perception, extending concepts to new contexts, even those unlinked to perceptual entities (Mitchell 2021; Dehaene et al. 2022). These capabilities are crucial for a wide range of significant cognitive functions.

The third principle concerns the concept of internalization. What makes the dual-loop model special is the presence of the two lateral hubs that allow for a closed loop, where sequences can move back and forth. This unique anatomy allows for computations that are independent of external data—truly internal computations (Weiller et al. 2022). The configuration enables us to covertly simulate our actions (dorsal) and compare them with abstract notions (ventral) in the context of planning (anterior) and sensory perception (posterior). For instance, motor imagery emerges from "off-line" simulations within sensorimotor networks that normally serve implicit "on-line" motor planning and control, grounding higher-order cognitive processes in simulated interactions with the environment (Hesslow 2002). Predictive feed-forward and feedback mechanisms that use input–output functions based on prelearned sensorimotor associations, binding perceptive states and goals to potential actions (inverse models) and motor plans to potential action effects (forward models) represent a common operational principle of the dorsal system (Vry et al. 2012). The ventral system supports cognitive control and conscious retrieval of off-line simulations situated in the dorsal system. The dorsal network, however, works automatically and implicitly, as these processing

steps are usually not consciously accessible (Sirigu et al. 2004). Awareness is reached only when a mismatch between predicted and actual states exceeds a certain level, when the planning of a complex or novel movement requires supervisory attention (Shallice and Burgess 1996). Comparable mechanisms may be observed in the medial dual loop for integration of appraisal with memory during the exhilaration of an eagerly awaited reunion.

Contemporary theories suggest that the DMN is insulated from the external world, which allows it to support perceptually decoupled states as in mind wandering (Mason et al. 2007; Buckner and DiNicola 2019). Internalization facilitates the generation of mental imagery (Spagna et al. 2021) and reasoning independently of sensory input, thus paving the way for foresight, anticipation, or even remorse and introspection. Our hubs align with the areas identified as encoding reward-based evidence that supports the most advantageous counterfactual alternative for upcoming decisions, as demonstrated in an fMRI study (Boorman et al. 2011). The "first person perspective," commonly associated with the precuneus (Lyu et al. 2023), necessitates the frontal lobe for the sense of "self-agency" (Simons et al. 2022; Johnson 2025). Self-awareness is characterized by the synchronous, harmonious activation of several spatially distant areas in both anterior and posterior regions, to form a single, brain-scale workspace (Dehaene and Naccache 2001). The hubs further have the capability to accumulate and synthesize information over minutes-long timescales, as seen in narratives, thereby binding "temporally" separated data into a coherent understanding (Hahamy et al. 2023). The hubs are also the core brain system that mediates mental time traveling (Schacter et al. 2007), which requires a subjective awareness of time (autonoesis) (Fabbro et al. 2015). Self-organizing systems are crucial for individual identity and subjectivity. We have to decouple ourselves from the moment to be able to place ourselves in time. In patients in a vegetative or minimally conscious state, the connectivity within the resting state network of these four anatomical hubs inversely correlates with the degree of consciousness (Giacino et al. 2014).

The fourth principle of the meta-loop involves integrating and balancing internal representations of both the internal and the extrapersonal world. Evidence suggests that the interaction between medial and lateral brain systems plays a crucial role in mind–body dynamics, supporting allostasis and interoception. Studies involving the retrograde transneuronal transport of the rabies virus in rats, task-based fMRI, and positron emission tomography, as well as rsfMRI and DTI, indicate that the autonomic brain network relies on cortical and subcortical structures, along with connecting tracts that belong to the medial and lateral systems (Benarroch 1993; Levinthal and Strick 2020; Reisert et al. 2021). These systems are embedded within cognitive processes and emotions (Benarroch 1993; Coenen et al. 2022). Allostasis necessitates predictive and perceptive inference to model the world within lateral and medial brain systems (Kleckner et al. 2017; Schulkin and Sterling 2019; Bettinger and Friston 2023). The meta-loop integrates these brain systems, each possessing internalized circuits for prediction through a combination of perceptual and active inference. Kleckner et al., using a combination of tract tracing studies in nonhuman primates, rsfMRI in humans, and brain–behavior evidence, described a brain system fundamental to allostasis and interoception (Kleckner et al. 2017). The regions are classified in terms of the DMN and SAL and correspond with the anatomical hubs identified in our study. The concept of allostasis can be generalized as integrated "brain–body dynamics," incorporating social, psychological, and environmental influences (Bettinger and Friston 2023). The

combination of external and internal worlds is also required to communicate with others about our emotions, ideas, or things not currently present, as well as to discuss past and future events. Additionally, it enables the accumulation of experience, knowledge, and understanding shaped by the interactions between individuals. We are capable of transmitting original thoughts to others, who, in turn, can ponder upon and further evolve the idea. Through the use of communicative tools such as speech or writing, a cultural memory is established (Dor 2015). Moreover, the blending of internal and external worlds is essential for the development of moral values, empathy, and the ToM. Functional MRI studies have shown the involvement of the same four central hubs in moral judgment and empathy (Pascual et al. 2013). Moral reasoning encompasses both the ability to view situations from others' perspectives and to grasp their emotions. In our analysis of the HCP behavioral data, the strength of anatomical conjunction on an individual level was associated with ToM task performance in both dual loops. The four hubs are the shared regions activated across all theory of mind tasks, as identified through an activation likelihood estimation analysis across 144 fMRI study datasets (Molenberghs et al. 2016). The capacity to ascribe mental states to others and the development of morality evolve over the years. Tract-based spatial statistics and probabilistic tractography have demonstrated that a developmental milestone in understanding false beliefs around the age of four correlates with changes in the local white matter structure at the hubs in the inferior frontal gyrus, middle temporal gyrus, medial prefrontal cortex, and posterior cingulate cortex (Grosse Wiesmann et al. 2017). This corresponds to the findings of Flechsig (Fig. 6). In individuals with autism spectrum disorder, particularly those with deficits in social cognition and ToM, structural and functional alterations at these hubs have been observed in fMRI studies, alongside variations in cortical thickness and anomalies in both functional and structural connectivity (Molenberghs et al. 2016; Guo et al. 2023). It appears that allostasis, self-reference, and ToM are based on the same fundamental yet comprehensive anatomical structure.

The four architectural principles delineate the groundwork for a range of distinct skills such as analogy-making, ToM, teaching, cultural memory, and individual communication—abilities that are suggested to distinguish humans (Dehaene et al. 2022). The meta-loop represents an impressively straightforward anatomical framework, offering a theoretically and anatomically robust assortment of hubs and connections, which may, in the future, be employed to interpret dynamic rsfMRI or electroencephalogram (EEG) data, including longitudinal analyses. The anatomical conjunction strength within these nodes can be correlated with behavioral patterns. This model aids in comprehending neurological, neuropsychological, and psychiatric symptomatology, and it assists in developing hypotheses regarding recovery from damage as well as in predicting responses to treatments or interventions.

Acknowledgments

Author contributions

Cornelius Weiller (Conceptualization, Data curation, Funding acquisition, Investigation, Methodology, Project administration, Supervision, Visualization), Marco Reisert (Data curation, Formal analysis, Investigation, Visualization), Pierre LeVan (Investigation), Jonas Hosp (Visualization), Volker Arnd Coenen (Conceptualization), and Michel Rijntjes (Conceptualization, Visualization).

Supplementary material

Supplementary material is available at *Cerebral Cortex* online.

Funding

Data availability

This paper analyses existing, publicly available data. This paper does not report original code. Any additional information required to reanalyze the data reported in this paper is available from the corresponding author upon request.

References

Amunts K, Mohlberg H, Bludau S, Zilles K. 2020. Julich-Brain: a 3D probabilistic atlas of the human brain's cytoarchitecture. *Science*. 369:988–992. https://doi.org/10.1126/science.abb4588.

Assem M, Shashidhara S, Glasser MF, Duncan J. 2025. *Category-biased patches encircle core domain-general regions in the human lateral prefrontal cortex*. bioRxiv [Preprint]. January 16, 2025. https://doi.org/10.1101/2025.01.16.633461.

Benarroch EE. 1993. The central autonomic network: functional organization, dysfunction, and perspective. *Mayo Clin Proc*. 68: 988–1001. https://doi.org/10.1016/S0025-6196(12)62272-1.

Benjamini Y, Hochberg Y. 1995. Controlling the false discovery rate: a practical and powerful approach to multiple testing. *J R Stat Soc Ser B Methodol*. 57:289–300. https://doi.org/10.1111/j.2517-6161.1995.tb02031.x.

Benzinger TLS et al. 2013. Regional variability of imaging biomarkers in autosomal dominant Alzheimer's disease. *Proc Natl Acad Sci USA*. 110:E4502–E4509. https://doi.org/10.1073/pnas.1317918110.

Bettinger JS, Friston KJ. 2023. Conceptual foundations of physiological regulation incorporating the free energy principle and self-organized criticality. *Neurosci Biobehav Rev*. 155:105459. https://doi.org/10.1016/j.neubiorev.2023.105459.

Binder JR, Desai RH, Graves WW, Conant LL. 2009. Where is the semantic system? A critical review and meta-analysis of 120 functional neuroimaging studies. *Cereb Cortex*. 19:2767–2796. https://doi.org/10.1093/cercor/bhp055.

Blumenthal-Dramé A et al. 2017. Frequency and chunking in derived words: a parametric fMRI study. *J Cogn Neurosci*. 29:1162–1177. https://doi.org/10.1162/jocn_a_01120.

Boorman ED, Behrens TE, Rushworth MF. 2011. Counterfactual choice and learning in a neural network centered on human lateral frontopolar cortex. *PLoS Biol*. 9:e1001093. https://doi.org/10.1371/journal.pbio.1001093.

Bracht T et al. 2009. Extraction of prefronto-amygdalar pathways by combining probability maps. *Psychiatry Res Neuroimaging*. 174: 217–222. https://doi.org/10.1016/j.pscychresns.2009.05.001.

Brodal P. 2004. *The central nervous system: structure and function*. USA: Oxford University Press.

Brodt S et al. 2018. Fast track to the neocortex: a memory engram in the posterior parietal cortex. *Science*. 362:1045–1048. https://doi.org/10.1126/science.aau2528.

Broulidakis MJ, Golm D, Cortese S, Fairchild G, Sonuga-Barke E. 2022. Default mode network connectivity and attention-deficit/hyperactivity disorder in adolescence: associations with delay aversion and temporal discounting, but not mind wandering. *Int J Psychophysiol*. 173:38–44. https://doi.org/10.1016/j.ijpsycho.2022.01.007.

Buckner RL, DiNicola LM. 2019. The brain's default network: updated anatomy, physiology and evolving insights. *Nat Rev Neurosci*. 20: 593–608. https://doi.org/10.1038/s41583-019-0212-7.

Buckner RL et al. 2009. Cortical hubs revealed by intrinsic functional connectivity: mapping, assessment of stability, and relation to Alzheimer's disease. *J Neurosci*. 29:1860–1873. https://doi.org/10.1523/JNEUROSCI.5062-08.2009.

Bullmore E, Sporns O. 2012. The economy of brain network organization. *Nat Rev Neurosci*. 13:336–349. https://doi.org/10.1038/nrn3214.

Castrillon G et al. 2023. An energy costly architecture of neuro-modulators for human brain evolution and cognition. *Sci Adv*. 9:eadi7632. https://doi.org/10.1126/sciadv.adi7632.

Catani M et al. 2013. A novel frontal pathway underlies verbal fluency in primary progressive aphasia. *Brain*. 136:2619–2628. https://doi.org/10.1093/brain/awt163.

Chand GB, Wu J, Hajjar I, Qiu D. 2017. Interactions of the salience network and its subsystems with the default-mode and the central-executive networks in normal aging and mild cognitive impairment. *Brain Connect*. 7:401–412. https://doi.org/10.1089/brain.2017.0509.

Coenen VA et al. 2022. "The heart asks pleasure first"-conceptualizing psychiatric diseases as MAINTENANCE network dysfunctions through insights from slMFB DBS in depression and obsessive-compulsive disorder. *Brain Sci*. 12:438. https://doi.org/10.3390/brainsci12040438.

Corbetta M, Shulman GL. 2002. Control of goal-directed and stimulus-driven attention in the brain. *Nat Rev Neurosci*. 3: 201–215. https://doi.org/10.1038/nrn755.

Damoiseaux JS et al. 2006. Consistent resting-state networks across healthy subjects. *Proc Natl Acad Sci USA*. 103:13848–13853. https://doi.org/10.1073/pnas.0601417103.

Deco G, Jirsa VK, McIntosh AR. 2011. Emerging concepts for the dynamical organization of resting-state activity in the brain. *Nat Rev Neurosci*. 12:43–56. https://doi.org/10.1038/nrn2961.

Dehaene S, Naccache L. 2001. Towards a cognitive neuroscience of consciousness: basic evidence and a workspace framework. *Cognition*. 79:1–37. https://doi.org/10.1016/S0010-0277(00)00123-2.

Dehaene S, Al Roumi F, Lakretz Y, Planton S, Sablé-Meyer M. 2022. Symbols and mental programs: a hypothesis about human singularity. *Trends Cogn Sci*. 26:751–766. https://doi.org/10.1016/j.tics.2022.06.010.

Dehghani M et al. 2017. Decoding the neural representation of story meanings across languages. *Hum Brain Mapp*. 38:6096–6106. https://doi.org/10.1002/hbm.23814.

Dor D. 2015. *The instruction of imagination: language as a social communication technology*. Oxford: Oxford University Press, https://doi.org/10.1093/acprof:oso/9780190256623.001.0001.

Du J et al. 2024. Organization of the human cerebral cortex estimated within individuals: networks, global topography, and function. *J Neurophysiol*. 131:1014–1082. https://doi.org/10.1152/jn.00308.2023.

Duncan J. 2010. The multiple-demand (MD) system of the primate brain: mental programs for intelligent behaviour. *Trends Cogn Sci*. 14:172–179. https://doi.org/10.1016/j.tics.2010.01.004.

Ereira S, Waters S, Razi A, Marshall CR. 2024. Early detection of dementia with default-mode network effective connectivity. *Nat Mental Health*. 2:787–800. https://doi.org/10.1038/s44220-024-00259-5.

Fabbro F, Aglioti SM, Bergamasco M, Clarici A, Panksepp J. 2015. Evolutionary aspects of self- and world consciousness in vertebrates. *Front Hum Neurosci*. 9:175. https://doi.org/10.3389/fnhum.2015.00157.

Fillard P et al. 2011. Quantitative evaluation of 10 tractography algorithms on a realistic diffusion MR phantom. *NeuroImage*. 56:220–234. https://doi.org/10.1016/j.neuroimage.2011.01.032.

Fitch WT. 2014. Toward a computational framework for cognitive biology: unifying approaches from cognitive neuroscience and comparative cognition. *Phys Life Rev*. 11:329–364. https://doi.org/10.1016/j.plrev.2014.04.005.

Flechsig P. 1920. *Anatomie des menschlichen Gehirns und Rückenmarks auf myelogenetischer Grundlage*. Leipzig: Thieme.

Freedman DJ, Riesenhuber M, Poggio T, Miller EK. 2001. Categorical representation of visual stimuli in the primate prefrontal cortex. *Science*. 291:312–316. https://doi.org/10.1126/science.291.5502.312.

Friston K. 2010. The free-energy principle: a unified brain theory? *Nat Rev Neurosci*. 11:127–138. https://doi.org/10.1038/nrn2787.

Fuster JM. 2004. Upper processing stages of the perception-action cycle. *Trends Cogn Sci*. 8:143–145. https://doi.org/10.1016/j.tics.2004.02.004.

García-Cabezas MÁ, Zikopoulos B, Barbas H. 2019. The structural model: a theory linking connections, plasticity, pathology, development and evolution of the cerebral cortex. *Brain Struct Funct*. 224:985–1008. https://doi.org/10.1007/s00429-019-01841-9.

Gentner D. 1983. Structure-mapping: a theoretical framework for analogy. *Cogn Sci*. 7:155–170.

Geranmayeh F, Leech R, Wise RJS. 2016. Network dysfunction predicts speech production after left hemisphere stroke. *Neurology*. 86:1296–1305. https://doi.org/10.1212/WNL.0000000000002537.

Giacino JT, Fins JJ, Laureys S, Schiff ND. 2014. Disorders of consciousness after acquired brain injury: the state of the science. *Nat Rev Neurol*. 10:99–114. https://doi.org/10.1038/nrneurol.2013.279.

Glasser MF et al. 2013. The minimal preprocessing pipelines for the human connectome project. *NeuroImage*. 80:105–124. https://doi.org/10.1016/j.neuroimage.2013.04.127.

Goldstein K. 1925. Das Symptom, seine Entstehung und Bedeutung für unsere Auffassung vom Bau und von der Funktion des Nervensystems. *Archiv für Psychiatrie*. 76:84–108. https://doi.org/10.1007/BF01814686.

Grosse Wiesmann C, Schreiber J, Singer T, Steinbeis N, Friederici AD. 2017. White matter maturation is associated with the emergence of theory of mind in early childhood. *Nat Commun*. 8:14692. https://doi.org/10.1038/ncomms14692.

Guo X et al. 2023. Dysregulated dynamic time-varying triple-network segregation in children with autism spectrum disorder. *Cereb Cortex*. 33:5717–5726. https://doi.org/10.1093/cercor/bhac454.

Hahamy A, Dubossarsky H, Behrens TEJ. 2023. The human brain reactivates context-specific past information at event boundaries of naturalistic experiences. *Nat Neurosci*. 26:1080–1089. https://doi.org/10.1038/s41593-023-01331-6.

Hesslow G. 2002. Conscious thought as simulation of behaviour and perception. *Trends Cogn Sci*. 6:242–247. https://doi.org/10.1016/S1364-6613(02)01913-7.

Hill J et al. 2010. Similar patterns of cortical expansion during human development and evolution. *Proc Natl Acad Sci*. 107:13135–13140. https://doi.org/10.1073/pnas.1001229107.

Hofstadter D, Sander E. 2013. *Surfaces and essences: analogy as the fuel and fire of thinking*. New York: Basic Books.

Jagust WJ, Mormino EC. 2011. Lifespan brain activity, β-amyloid, and Alzheimer's disease. *Trends Cogn Sci*. 15:520–526. https://doi.org/10.1016/j.tics.2011.09.004.

Johnson MK. 2025. Reflecting on the origins of subjective experience. *Annu Rev Psychol*. 76:1–28. https://doi.org/10.1146/annurev-psych-062424-112106.

Jones EG, Powell TPS. 1970. An anatomical study of converging sensory pathways within the cerebral cortex of the monkey. *Brain*. 93:793–820. https://doi.org/10.1093/brain/93.4.793.

Jones DK, Christiansen KF, Chapman RJ, Aggleton JP. 2013. Distinct subdivisions of the cingulum bundle revealed by diffusion MRI fibre tracking: implications for neuropsychological investigations. *Neuropsychologia*. 51:67–78. https://doi.org/10.1016/j.neuropsychologia.2012.11.018.

Klauer KJ, Willmes K, Phye GD. 2002. Inducing inductive reasoning: does it transfer to fluid intelligence? *Contemp Educ Psychol*. 27:1–25. https://doi.org/10.1006/ceps.2001.1079.

Kleckner IR et al. 2017. Evidence for a large-scale brain system supporting Allostasis and Interoception in humans. *Nat Hum Behav*. 1:0069. https://doi.org/10.1038/s41562-017-0069.

Kravitz DJ, Saleem KS, Baker CI, Ungerleider LG, Mishkin M. 2013. The ventral visual pathway: an expanded neural framework for the processing of object quality. *Trends Cogn Sci*. 17:26–49. https://doi.org/10.1016/j.tics.2012.10.011.

Kristensen LB, Wang L, Petersson KM, Hagoort P. 2013. The interface between language and attention: prosodic focus marking recruits a general attention network in spoken language comprehension. *Cereb Cortex*. 23:1836–1848. https://doi.org/10.1093/cercor/bhs164.

Kwon YH et al. 2025. Situating the salience and parietal memory networks in the context of multiple parallel distributed networks using precision functional mapping. *Cell Rep*. 44:115207. https://doi.org/10.1016/j.celrep.2024.115207.

Lee Y, Chahal R, Gotlib IH. 2024. The default mode network is associated with changes in internalizing and externalizing problems differently in adolescent boys and girls. *Dev Psychopathol*. 36:834–843. https://doi.org/10.1017/S0954579423000111.

Levinthal DJ, Strick PL. 2020. Multiple areas of the cerebral cortex influence the stomach. *Proc Natl Acad Sci*. 117:13078–13083. https://doi.org/10.1073/pnas.2002737117.

Lombardo D, Kaufmann T. 2023. Different patterns of intrinsic functional connectivity at the default mode and attentional networks predict crystalized and fluid abilities in childhood. *Cereb Cortex Commun*. 4:tgad015. https://doi.org/10.1093/texcom/tgad015.

Luppi AI et al. 2022. A synergistic core for human brain evolution and cognition. *Nat Neurosci*. 25:771–782. https://doi.org/10.1038/s41593-022-01070-0.

Lyu D et al. 2023. Causal evidence for the processing of bodily self in the anterior precuneus. *Neuron*. 111:2502–2512.e4. https://doi.org/10.1016/j.neuron.2023.05.013.

Macko KA et al. 1982. Mapping the primate visual system with (2-14C) deoxyglucose. *Science*. 218:394–397. https://doi.org/10.1126/science.7123241.

MacLean PD. 1955. The limbic system ("visceral brain") in relation to central Gray and reticulum of the brain stem. *Psychosom Med*. 17:355–366. https://doi.org/10.1097/00006842-195509000-00003.

Mai JK, Majtanik M. 2017. *Human brain in standard MNI space: a comprehensive pocket atlas*. San Diego: Academic Press: Elsevier.

Makris N et al. 2017. Mapping temporo-parietal and temporo-occipital cortico-cortical connections of the human middle longitudinal fascicle in subject-specific, probabilistic, and stereotaxic Talairach spaces. *Brain Imaging Behav*. 11:1258–1277. https://doi.org/10.1007/s11682-016-9589-3.

Margulies DS et al. 2016. Situating the default-mode network along a principal gradient of macroscale cortical organization. *Proc Natl Acad Sci USA*. 113:12574–12579. https://doi.org/10.1073/pnas.1608282113.

Martin A, Wiggs CL, Ungerleider LG, Haxby JV. 1996. Neural correlates of category-specific knowledge. *Nature*. 379:649–652. https://doi.org/10.1038/379649a0.

Mason MF et al. 2007. Wandering minds: the default network and stimulus-independent thought. *Science (New York, NY)*. 315:393–395. https://doi.org/10.1126/science.1131295.

Medendorp WP. 2011. Spatial constancy mechanisms in motor control. *Philos Trans R Soc Lond Ser B Biol Sci*. 366:476–491. https://doi.org/10.1098/rstb.2010.0089.

Menon V. 2011. Large-scale brain networks and psychopathology: a unifying triple network model. *Trends Cogn Sci*. 15:483–506. https://doi.org/10.1016/j.tics.2011.08.003.

Menon V. 2023. 20 years of the default mode network: a review and synthesis. *Neuron*. 111:2469–2487. https://doi.org/10.1016/j.neuron.2023.04.023.

Mesulam MM. 1987. *Principles of behavioral neurology*. 3rd ed. Philadelphia: F.A.Davis Company.

Mitchell M. 2021. Abstraction and analogy-making in artificial intelligence. *Ann N Y Acad Sci*. 1505:79–101. https://doi.org/10.1111/nyas.14619.

Molenberghs P, Johnson H, Henry JD, Mattingley JB. 2016. Understanding the minds of others: a neuroimaging meta-analysis. *Neurosci Biobehav Rev*. 65:276–291. https://doi.org/10.1016/j.neubiorev.2016.03.020.

Nieuwenhuys R, Puelles L. 2016. *Towards a new Neuromorphology*. Heidelberg, New York, Dordrecht, London: Springer, https://doi.org/10.1007/978-3-319-25693-1.

Oishi K et al. 2008. Human brain white matter atlas: identification and assignment of common anatomical structures in superficial white matter. *NeuroImage*. 43:447–457. https://doi.org/10.1016/j.neuroimage.2008.07.009.

Pang JC et al. 2023. Geometric constraints on human brain function. *Nature*. 618:566–574. https://doi.org/10.1038/s41586-023-06098-1.

Papez JW. 1937. A proposed mechanism of emotion. *Arch Neurol Psychiatr*. 38:725–743. https://doi.org/10.1001/archneurpsyc.1937.02260220069003.

Park H-J, Friston K. 2013. Structural and functional brain networks: from connections to cognition |. *Science*. 342:1238411. https://doi.org/10.1126/science.1238411.

Pascual L, Gallardo-Pujol D, Rodrigues P. 2013. How does morality work in the brain? A functional and structural perspective of moral behavior. *Front Integr Neurosci*. 7:65. https://doi.org/10.3389/fnint.2013.00065.

Passingham RE. 2021. *Understanding the prefrontal cortex: selective advantage, connectivity, and neural operations, Oxford psychology series*. Oxford, New York: Oxford University Press, https://doi.org/10.1093/oso/9780198844570.001.0001.

Petrides M, Pandya D. 2012. The frontal cortex. In: Mai J, Paxinos G, editors. *The human nervous system*. 3rd. ed. San Diego: Elsevier Academic Press. p. 988–1011, https://doi.org/10.1016/B978-0-12-374236-0.10026-4.

Puelles L, Alonso A, García-Calero E, Martínez-de-la-Torre M. 2019. Concentric ring topology of mammalian cortical sectors and relevance for patterning studies. *J Comp Neurol*. 527:1731–1752. https://doi.org/10.1002/cne.24650.

Raichle ME. 2015. The brain's default mode network. *Annu Rev Neurosci*. 38:433–447. https://doi.org/10.1146/annurev-neuro-071013-014030.

Rauschecker JP. 2018. Where, when, and how: are they all sensorimotor? Towards a unified view of the dorsal pathway in vision and audition. *Cortex*. 98:262–268. https://doi.org/10.1016/j.cortex.2017.10.020.

Reisert M et al. 2011. Global fiber reconstruction becomes practical. *NeuroImage*. 54:955–962. https://doi.org/10.1016/j.neuroimage.2010.09.016.

Reisert M, Weiller C, Hosp JA. 2021. Displaying the autonomic processing network in humans - a global tractography approach. *NeuroImage*. 231:117852. https://doi.org/10.1016/j.neuroimage.2021.117852.

Rijntjes M et al. 1999. A blueprint for movement: functional and anatomical representations in the human motor system. *J Neurosci*. 19:8043–8048. https://doi.org/10.1523/JNEUROSCI.19-18-08043.1999.

Rizzolatti G, Fadiga L, Fogassi L, Gallese V. 1997. The space around us [see comments]. *Science*. 277:190–191. https://doi.org/10.1126/science.277.5323.190.

Rolls ET. 2015. Limbic systems for emotion and for memory, but no single limbic system. *Cortex*. 62:119–157. https://doi.org/10.1016/j.cortex.2013.12.005.

Romanski LM et al. 1999. Dual streams of auditory afferents target multiple domains in the primate prefrontal cortex. *Nat Neurosci*. 2:1131–1136. https://doi.org/10.1038/16056.

Sakreida K et al. 2016. Affordance processing in segregated parieto-frontal dorsal stream sub-pathways. *Neurosci Biobehav Rev*. 69:89–112. https://doi.org/10.1016/j.neubiorev.2016.07.032.

Saris IMJ et al. 2020. Default mode network connectivity and social dysfunction in major depressive disorder. *Sci Rep*. 10:194. https://doi.org/10.1038/s41598-019-57033-2.

Saur D et al. 2008. Ventral and dorsal pathways for language. *Proc Natl Acad Sci*. 105:18035–18040. https://doi.org/10.1073/pnas.0805234105.

Sayalı C, Badre D. 2019. Neural systems of cognitive demand avoidance. *Neuropsychologia*. 123:41–54. https://doi.org/10.1016/j.neuropsychologia.2018.06.016.

Schacter DL, Addis DR, Buckner RL. 2007. Remembering the past to imagine the future: the prospective brain. *Nat Rev Neurosci*. 8:657–661. https://doi.org/10.1038/nrn2213.

Schmahmann JD, Pandya D. 2006. *Fiber pathways of the brain*. Oxford: Oxford University Press.

Schulkin J, Sterling P. 2019. Allostasis: A brain-centered, predictive mode of physiological regulation. *Trends Neurosci*. 42:740–752. https://doi.org/10.1016/j.tins.2019.07.010.

Schumacher LV et al. 2018. Probing the reproducibility of quantitative estimates of structural connectivity derived from global tractography. *NeuroImage*. 175:215–229. https://doi.org/10.1016/j.neuroimage.2018.01.086.

Schurz M, Radua J, Aichhorn M, Richlan F, Perner J. 2014. Fractionating theory of mind: a meta-analysis of functional brain imaging studies. *Neurosci Biobehav Rev*. 42:9–34. https://doi.org/10.1016/j.neubiorev.2014.01.009.

Schwartz E et al. 2023. Evolution of cortical geometry and its link to function, behaviour and ecology. *Nat Commun*. 14:2252. https://doi.org/10.1038/s41467-023-37574-x.

Seeley WW. 2019. The salience network: a neural system for perceiving and responding to homeostatic demands. *J Neurosci*. 39:9878–9882. https://doi.org/10.1523/JNEUROSCI.1138-17.2019.

Shallice T, Burgess P. 1996. The domain of supervisory processes and temporal organization of behaviour. *Philos Trans R Soc Lond Ser B Biol Sci* 351:1405–1411; discussion 1411–1412. https://doi.org/10.1098/rstb.1996.0124.

Sheth BR, Young R. 2016. Two visual pathways in primates based on sampling of space: exploitation and exploration of visual information. *Front Integr Neurosci*. 10:37. https://doi.org/10.3389/fnint.2016.00037.

Shirer WR, Ryali S, Rykhlevskaia E, Menon V, Greicius MD. 2012. Decoding subject-driven cognitive states with whole-brain connectivity patterns. *Cereb Cortex*. 22:158–165. https://doi.org/10.1093/cercor/bhr099.

Simons JS, Ritchey M, Fernyhough C. 2022. Brain mechanisms underlying the subjective experience of remembering. *Annu Rev Psychol*. 73:159–186. https://doi.org/10.1146/annurev-psych-030221-025439.

Sirigu A et al. 2004. Altered awareness of voluntary action after damage to the parietal cortex. *Nat Neurosci*. 7:80–84. https://doi.org/10.1038/nn1160.

Smith SM et al. 2013. Resting-state fMRI in the human connectome project. *NeuroImage*. 80:144–168. https://doi.org/10.1016/j.neuroimage.2013.05.039.

Spagna A, Hajhajate D, Liu J, Bartolomeo P. 2021. Visual mental imagery engages the left fusiform gyrus, but not the early visual cortex: a meta-analysis of neuroimaging evidence. *Neurosci Biobehav Rev*. 122:201–217. https://doi.org/10.1016/j.neubiorev.2020.12.029.

Spreng RN, Grady CL. 2010. Patterns of brain activity supporting autobiographical memory, prospection, and theory of mind, and their relationship to the default mode network. *J Cogn Neurosci*. 22:1112–1123. https://doi.org/10.1162/jocn.2009.21282.

Thiebaut de Schotten M, Forkel SJ. 2022. The emergent properties of the connected brain. *Science*. 378:505–510. https://doi.org/10.1126/science.abq2591.

Tucker DM, Luu P. 2023. Adaptive control of functional connectivity: dorsal and ventral limbic divisions regulate the dorsal and ventral neocortical networks. *Cereb Cortex*. 33:7870–7895. https://doi.org/10.1093/cercor/bhad085.

Ungerleider LG, Gaffan D, Pelak VS. 1989. Projections from inferior temporal cortex to prefrontal cortex via the uncinate fascicle in rhesus monkeys. *Exp Brain Res*. 76:473–484. https://doi.org/10.1007/BF00248903.

van den Hoven E et al. 2024. Time to bury the chisel: a continuous dorsal association tract system. *Brain Struct Funct*. 229:1527–1532. https://doi.org/10.1007/s00429-024-02829-w.

Vry M-S et al. 2012. Ventral and dorsal fiber systems for imagined and executed movement. *Exp Brain Res*. 219:203–216. https://doi.org/10.1007/s00221-012-3079-7.

Weiller C, Rijntjes M. 2023. Should concepts of brain functions be based on psychology or anatomy? An echo from Kurt Goldstein. *Brain*. 146:1234–1235. https://doi.org/10.1093/brain/awad081.

Weiller C et al. 2021. The ventral pathway of the human brain: a continuous association tract system. *NeuroImage*. 234:117977. https://doi.org/10.1016/j.neuroimage.2021.117977.

Weiller C, Reisert M, Glauche V, Musso M, Rijntjes M. 2022. The dual-loop model for combining external and internal worlds in our brain. *NeuroImage*. 263:119583. https://doi.org/10.1016/j.neuroimage.2022.119583.

Yeo BTT et al. 2011. The organization of the human cerebral cortex estimated by intrinsic functional connectivity. *J Neurophysiol*. 106:1125–1165. https://doi.org/10.1152/jn.00338.2011.

Zhang J et al. 2019. Intrinsic functional connectivity is organized as three interdependent gradients. *Sci Rep*. 9:15976.